Efficient laser action of Yb:LSO and Yb:YSO oxyorthosilicates crystals under high-power diode-pumping

Mathieu Jacquemet, Cyrille Jacquemet, N. Janel, Frédéric Druon, François Balembois, Patrick Georges, J. Petit, Bruno Viana, D. Vivien, Bernard Ferrand

HAL Id: hal-00709959

https://hal-iogs.archives-ouvertes.fr/hal-00709959

Submitted on 11 Aug 2023

Efficient laser action of Yb:LSO and Yb:YSO oxyorthosilicates crystals under high-power diode-pumping

M. Jacquemet[1], C. Jacquemet[1], N. Janel[1], F. Druon[1], F. Balembois[1], P. Georges[1], J. Petit[2], B. Viana[2], D. Vivien[2], B. Ferrand[3]

[1] Laboratoire Charles Fabry de l'Institut d'Optique UMR 8501 du CNRS,
   Bât. 503 Centre Universitaire, 91403 Orsay Cedex, France
[2] Laboratoire de Chimie Appliquée de l'Etat Solide UMR 7574 du CNRS ENSCP,
   11, rue Pierre & Marie Curie, 75231 Paris Cedex 05, France
[3] LETI/DOPT/CEA-G, 17, Rue des Martyrs, 38054 Grenoble Cedex 9, France

ABSTRACT We report here on the efficient laser action of a new Yb-doped crystal Yb^{3+}:Lu_2SiO_5 (Yb:LSO) under high power diode-pumping (15 W). Its performances were compared to another Yb-doped crystal belonging to the oxyorthosilicate family: the Yb:YSO. For both crystals, more than 7 W of laser radiation around 1 μm was obtained under 14.4 W of incident pump power at 978 nm, leading to high optical conversions of more than 50%. Finally, both crystals demonstrate little sensitivity to pump wavelength drift and exhibit broad tunability at a multiwatt level (more than 4 W over 50 nm and 60 nm, respectively for Yb:LSO and Yb:YSO).

PACS 42.55.Xi; 42.60.Pk; 42.70.Hj

1   Introduction

Thanks to the development of high power InGaAs laser diodes in the 900–980 nm range, studies on Ytterbium-doped materials have led to a large number of new crystals, in the past ten years. Particularly, monoclinic double tungstates Yb:KYW and Yb:KGW [1, 2], vanadates $Yb:GdVO_4$ [3], fluoroapatites Yb:S-FAP and Yb:SYS [4, 5], borates Yb:GdCOB and Yb:BOYS [6, 7], garnet Yb:GGG [8], fluoride $Yb:CaF_2$ [9], or sesquioxides $Yb:Y_2O_3$, $Yb:Lu_2O_3$ and $Yb:Sc_2O_3$ [10, 11] appeared in addition to the well-known Yb:YAG. Unique properties of Yb-doped materials have already been exploited in different domains. As an example, kilowatt-class diode-pumped lasers recently made are based on small quantum defect (generally less than 10%), the absence of parasitic spectroscopic effects and the good thermal conductivity of Yb:YAG [12]. The broad emission band of a large number of Yb-doped crystals makes possible the realization of femtosecond oscillators [2, 5, 7] and amplifiers [13]. However, "ideal" Yb-doped crystal still does not exist: as an example, Yb:YAG suffers from a narrow and unpolarized emission band. Numerous Yb-doped materials have a relatively low thermal conductivity, generally below $3\,W\,m^{-1}\,K^{-1}$, limiting high power applications. Yb-sesquioxides are an issue to this latter problem, thanks to their high thermal conductivity when undoped [11]. However, they suffer from a somewhat difficult growth and relatively narrow emission spectrum.

In this paper, we present a new material, Yb:LSO, combining both high thermal conductivity and large tunability. The potential of this crystal is demonstrated in a very simple setup using a fiber-coupled laser diode (15 W at 978 nm) in end-pumping configuration, without any specific thermal management. Performances are compared to a more mature crystal from the same family Yb:YSO. One of the main ideas is that replacing the Yttrium ion with a Lutetium ion in a host matrix has the advantage of keeping a high thermal conductivity when doping with Ytterbium rare-earth ion, because of close molar masses between Yb and Lu.

2   Properties of Yb-doped oxyorthosilicates Yb:Y_2SiO_5 and Yb:Lu_2SiO_5

Oxyorthosilicates YSO and LSO are already used in a large photonic applications field, demonstrating that their growth is well-controlled. First, both are commonly used for scintillator applications when Ce-doped [14]. Moreover, the YSO host matrix is well-known since it has previously been doped with Neodymium and with Chromium as a laser material or as a saturable absorber [15–17]. Spectroscopic investigations and laser action have also been performed on Er,Yb:YSO [18]. Yb:YSO has already been tested under both Ti:Sa and low power diode pumping [19] and has specially been used for the development of a continuously diode-pumped tunable laser source between 1000 and 1010 nm [20]. However, no work has been reported under high-power diode-pumping (> 4 W).

2.1   *Thermo-optical properties*

Heat removal and thermal management in the gain media are the main limiting points concerning the development of efficient and high power laser systems. Obviously, limiting the quantum defect by pumping on the Zero-Line around 980 nm is the first way to decrease the thermal load into the Yb-doped crystal. Then, in order to have efficient heat removal, thermal conductivity has to be as high as possible. As a matter of fact, thermal conductivity generally decreases when the doping rate increases. This variation mostly depends on the molar mass difference between Ytterbium cation

and the substituted one (here, Y or Lu). The weaker the difference in molar mass is, the less the thermal conductivity decreases with Ytterbium concentration [22]. Using the simple model described in [22] by R. Gaumé et al., we calculated the thermal conductivity behavior with the Yb-doping rate (at. %), for Yb:LSO and Yb:YSO, in comparison with experimental measurements (see Fig. 1). Variations of the thermal conductivity of Yb:YAG, Yb:KGW and Yb:GdCOB with the Ytterbium concentration have also been calculated and are also presented. Experimental values for Yb:YAG can be found in [22], while average thermal conductivity of undoped KGW can be found in [23]. The only adjustable parameter for calculations is the thermal conductivity of the undoped host matrix.

Even if values are lower compared to Yb:YAG, thermal conductivity of undoped LSO and YSO are rather high among Yb-doped crystals with 5.3 and 4.4 W m^{-1} K^{-1}, respectively. In accordance with considerations in [22], good thermal conductivity can be obtained for crystals with high melting point temperature which is the case for YSO and LSO (around 2000 °C).

Furthermore, an important point is that Yb:LSO keeps almost its highest value when the doping rate increases. The undoped thermal conductivity of LSO has been adjusted to 5.31 W m^{-1} K^{-1} to fit correctly the experimental value of 5.3 W m^{-1} K^{-1} for the 8 at. % Yb^{3+}-doped LSO. Indeed, the mass difference, between Y and Yb, for Yb:YSO is around 50%, while it is less than 1% between Yb and Lu in Yb:LSO, explaining different behavior for both crystals. Calculations are in good agreement with experimental measurements, showing that Yb:LSO could be highly doped while keeping a really good thermal conductivity, comparable to Yb:YAG.

Spectroscopic investigations on Yb:Y$_2$SiO$_5$ and Yb:Lu$_2$SiO$_5$ have been presented in [21], showing that those two oxyorthosilicates laser crystals exhibit large splitting of the

$^2F_{7/2}$ ground state. This is an important issue to limit the thermal population of the terminal laser level and then to develop efficient laser systems. As previously said, two substitution sites for rare-earth doping ion exist in oxyorthosilicates host matrices. Depending on the substitution site, the overall splitting of the ground-state manifold $^2F_{7/2}$ is different, but remains high. Table 1 summarizes the $^2F_{7/2}$ splitting for Yb:LSO and Yb:YSO compared to three reference materials: Yb:YAG for kW output power sources, Yb:KGW for femtosecond applications [2], and Yb:GdCOB which has one of the highest ground-state splitting values.

Both Yb:LSO and Yb:YSO exhibit large splitting of the fundamental manifold, similar to those of Yb:YAG and Yb:GdCOB. It results in low thermal population of the terminal laser level in quasi-three levels laser operation, decreasing the laser threshold and reabsorption losses.

Therefore, Yb:LSO and Yb:YSO exhibit good thermal conductivity, particularly in regard to Yb:LSO, and important ground-state splitting, which makes them well-adapted for the development of high power laser systems.

2.2   Spectroscopic properties of Yb:Y$_2$SiO$_5$ and Yb:Lu$_2$SiO$_5$

Ytterbium-doped yttrium and lutetium oxyorthosilicate (Yb:YSO and Yb:LSO) are monoclinic positive biaxial crystals, grown by Czochralski technique at the CEA-LETI. The samples were 2-mm long, anti-reflection coated around 1 µm, 5 at. % and 8 at. % Yb-doped, respectively for Yb:YSO and Yb:LSO (9.2×10^{20} ions cm^{-3} and 15.6×10^{20} ions cm^{-3} respectively). Both samples used were cut with the n_Y axis along the propagation direction corresponding to the b direction of the crystalline matrix, which is also the growth axis. Following our convention for X, Y and Z cristallophysical axis, the X-axis corresponds to the lower refractive index (1.797 for Yb:LSO and 1.78 for Yb:YSO) while the Z-axis corresponds to the higher refractive index (1.825 for Yb:LSO and 1.811 for Yb:YSO).

Figure 2 shows the absorption and emission spectra of Yb:YSO and Yb:LSO at room temperature with respect to the available n_X and n_Z polarization axis.

Absorption spectra were recorded on a Varian Cary 5E double-beam spectrophotometer with a polarizer to characterize dependence of the polarization on the absorption. Emission spectra were carried out using a Ti:Sa laser beam at 900 nm for the excitation (Coherent 890). Luminescence was collected through an ARC SpectraPro 750 monochromator, detected by a PbS cell, cooled with liquid nitrogen, and recorded on a computer. We then derive the emission cross-sections from the room temperature fluorescence spectra and the Füchtbauer–Ladenburg relation.

Absorption and emission spectra of Yb:YSO and Yb:LSO exhibit almost the same shape. Both crystals exhibit main absorption peaks on the zero-line around 978 nm. They are

FIGURE 1   Calculated (*lines*) and experimental thermal conductivity values (*dots*) for Yb:YAG, Yb:KGW, Yb:GdCOB, Yb:LSO, and Yb:YSO versus Yb-doping rate (at. %)

Material	Yb:YAG	Yb:KGW	Yb:GdCOB [6]	Yb:LSO [21]	Yb:YSO [21]
$\Delta(^2F_{7/2})$ (cm^{-1})	785	535	1003	697 (I) - 971 (II)	715 (I) - 964 (II)

TABLE 1   Total splitting of the Yb^{3+} $^2F_{7/2}$ ground state in YAG, KGW, GdCOB, LSO and YSO
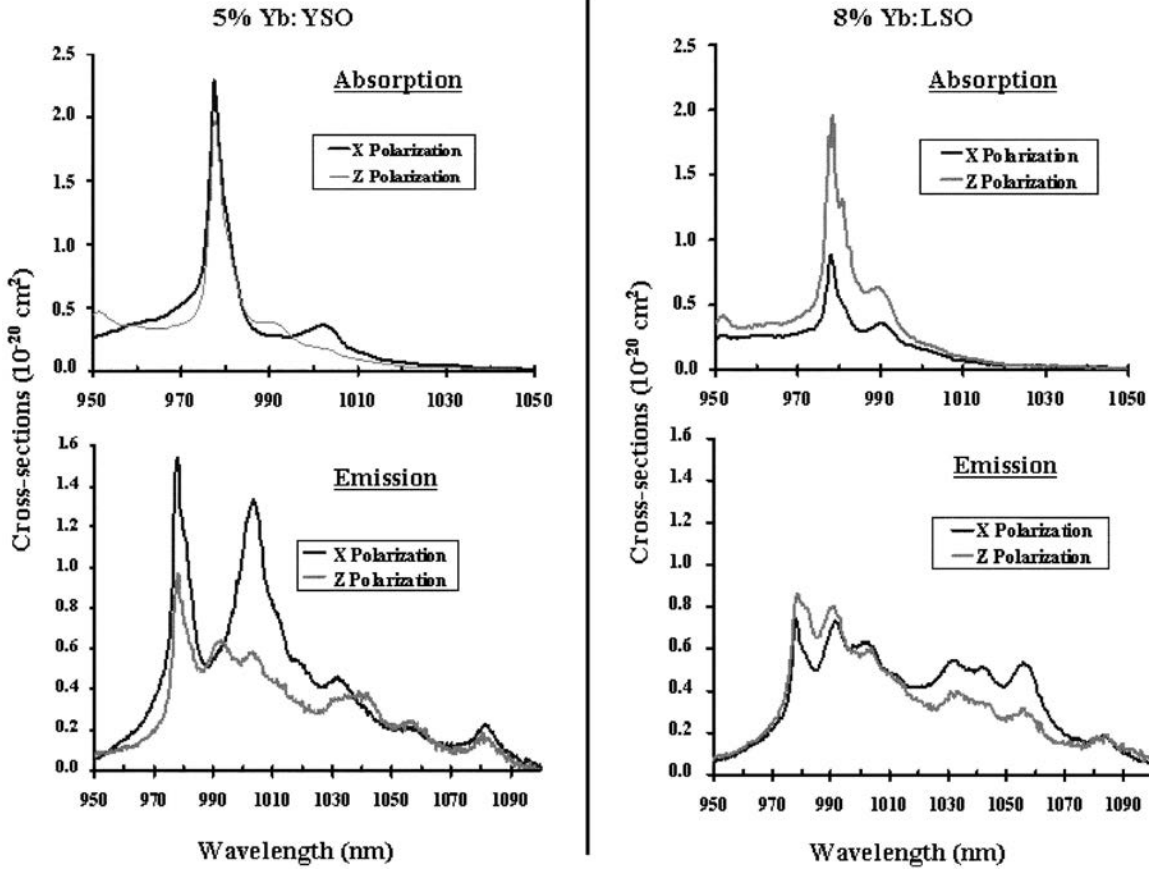
FIGURE 2 Absorption and emission spectra of a 5% Yb:YSO (*left*) and a 8% Yb:LSO (*right*) for both available axis

intense, more than two times greater than Yb:YAG, and well-adapted for diode-pumping since their line-width is about 3.5 nm for Yb:YSO and 4.5 nm for Yb:LSO (FWHM). Indeed, the typical line-width of our pump laser diode is about 2.5 nm (FWHM) leading to good spectral overlap and efficient energy transfer.

The emission spectra of Yb:YSO and Yb:LSO, in addition to the zero-line at 978 nm, are mainly composed of three bands around 1000, 1050 and 1080 nm. Around 1000 nm, despite the fact that emission cross-sections are high, the laser effect is not very efficient because of strong reabsorption losses due to thermal populating of the terminal laser level. Indeed, the energy difference between the fundamental pumping level and the terminal laser level is only few hundreds of cm^{-1} [20], which corresponds to the thermal energy $k_B T$ at room temperature. The second band around 1050 nm corresponds to an energy-level scheme where the terminal laser level is a little populated, but laser action is efficient although medium cross-sections. Finally, the last band around 1080 nm exhibits a terminal laser level very few populated. It makes low threshold and efficient laser systems, even if emission cross-sections are generally small. The main differences between both crystals spectra are the strong emission line around 1005 nm for Yb:YSO compared to Yb:LSO, and higher emission cross-sections for Yb:LSO around 1060 nm.

Experimental lifetime values of the excited manifold $^2F_{5/2}$ had been measured to be 0.67 ms for Yb:YSO and 0.95 ms for Yb:LSO [21].

3 Experimental setup

The pump source used in our experiments was a 15 W fiber-coupled laser diode emitting, around 978 nm, a nearly "top-hat" beam from a 200 µm core-diameter fiber with a numerical aperture of 0.22. The M^2 parameter of such a fiber-coupled laser diode had been measured to be 78 and its spectral linewidth was about 2.5 nm (FWHM). The experimental setup is shown on Fig. 3. The output of the fiber was relay-imaged into the crystal, by two 60 mm-focal length doublets, through the plane dichroic input mirror of the cavity (high transmission 980 nm, high reflection 1020–1200 nm). The cavity used was a V-shape three mirrors resonator composed of the plane input mirror, a concave folding mirror
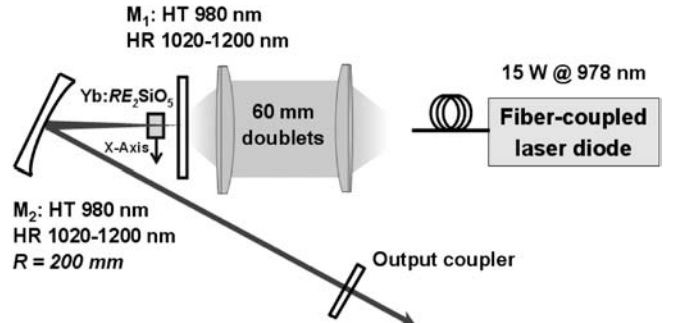

FIGURE 3 Experimental cavity setup

($R = 200$ mm–HT 980 nm-HR 1020–1200 nm) and a plane output coupler. Thus, the cavity beam waist was about 90 µm and, for a fixed pump spot size of 100 µm of radii, TEM_{00} oscillation mode was furthered.

This cavity setup allowed us to investigate the tuning range of each crystal by inserting a Lyot filter into the collimated arm of the cavity, between M_2 and the output coupler. Each crystal was directly side-pressed onto a copper mount, with thermal grease, and simply thermally water cooled around 20 °C. Both were placed with their X-axis polarization in the plane of the cavity (Z-axis perpendicular).

We took care to make all experiments under the same conditions for both crystals which means that we used exactly the same pump parameters (beam waist and power), the same cavity (lengths, angle of the folding mirror, position and orientation of the crystal . . .) and, for tunability tests, we used the same two plates Lyot filter located in the collimated arm. The maximum available incident pump power is 14.4 W at 978 nm and unpolarized, which means that the pump beam is, on average, half-and-half polarized along X and Z axis.

FIGURE 4 Laser performance in cw regime for 5% Yb:YSO (*solid curve*) and 8% Yb:LSO (*dashed curve*) at room temperature with a 4% transmission output coupler – *Inset*: Laser beam profile of Yb:LSO at maximum output power
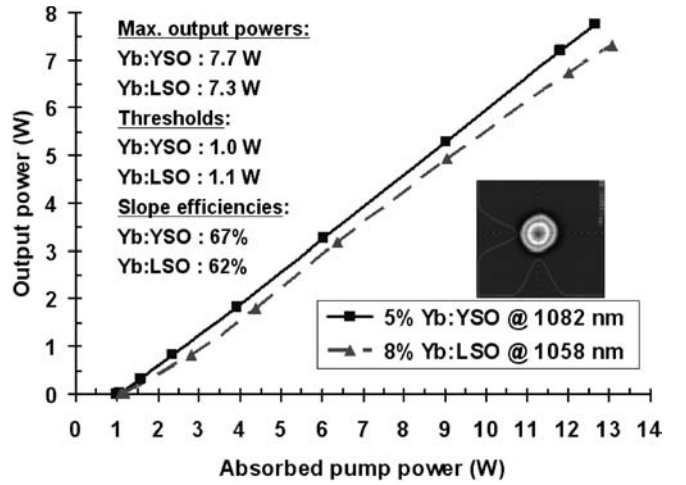
4 Comparison of the experimental results

In this section, we present a comparison of laser efficiencies obtained with both crystals as well as their tunability behavior using a Lyot filter. We also investigated the dependence of the laser power with pump wavelength by changing the temperature of the pump diode.

4.1 *Laser performance*

Under non-lasing conditions for each crystal, we measured the unsaturated absorption coefficient. With this aim, we used a low power pump beam (≈ 100 mW), at the optimum wavelength of 978 nm, with a spot size of about 2-mm in diameter. We measured 14.8 cm^{-1} for Yb:YSO and 15.5 cm^{-1} for Yb:LSO, corresponding to an unsaturated absorption of about 95%.

We performed laser experiments with various transmission values of the output coupler (2%, 4%, 6% and 10%) to obtain maximum output powers. For both crystals, best performance have been obtained for the same pump wavelength of about 978 nm, and also for the same output coupler with a transmission of 4%. In the following, we will only present best results corresponding to the 4% transmission output coupler. We took care to keep good laser beam quality (TEM_{00} beam profile) for all operations. The best laser performance is

presented on Fig. 4 as well as a summary of the main relevant values for both crystals.

Maximum output powers of 7.7 W and 7.3 W were obtained respectively for Yb:YSO and Yb:LSO, corresponding to optical-to-optical efficiencies of more than 53% and 50%. We measured almost the same threshold of about 1 W of absorbed pump power leading to great slope efficiencies values of 67% and 62% for Yb:YSO and Yb:LSO respectively. Furthermore, these performance had been obtained with good beam quality ($M^2 \approx 1.1$), as shown on Fig. 4 (inset) corresponding to the Yb:LSO laser beam at maximum output power.

In a quasi-three level laser system, the laser emission wavelength is not only fixed by the emission spectrum, but, also by reabsorption losses, according to the gain cross-section defined elsewhere [16]. In these experiments, both laser beams were polarized along their X-axis with laser wavelengths of 1082 nm and 1058 nm for Yb:YSO and Yb:LSO, respectively. Thus, for both crystals, the terminal level of the laser transition is one of the highest in energy among the ground-state manifold and is then few thermally populated.

It is also remarkable to notice that under lasing conditions and at maximum power, both crystals absorbed about 90% of the pump power, corresponding approximately to the unsaturated absorption regime under unlasing conditions. Indeed, after threshold, the laser effect is the predominant flow

Material	Yb:YAG	Yb:GGG	Yb:KGW	Yb:GdCOB	Yb:CaF$_2$	Yb:LSO	Yb:YSO
Maximum pump power (W)	12.9	14	4	13.5	15	14.4	14.4
Laser output power (W)	3.8	4.15	1.3	4.7	5.8	7.3	7.7
optical-to-optical efficiency (%)	29.5	29.6	32.5	34.8	38.7	50.7	53.5
Beam quality factor M^2	< 1.2	< 1.2	< 1.2	≈ 3.5	< 1.2	≈ 1.1	≈ 1.1
Reference	8	8	2	6	9	this work	this work

TABLE 2 Comparison of the cw performance of Yb-doped crystals under longitudinal diode-pumping

from the excited laser level to the terminal level of the laser transition, which increases significantly the population of the terminal level. Because of fast thermalization among $^2F_{7/2}$ manifold, the ground-state level becomes strongly populated leading to absorption values very close to the unsaturated absorption ones.

The obtained optical conversion efficiency values are very good when compared to some other Yb-doped crystals used in the same conditions, namely under single-pass end-pumping configuration on the Zero-Line absorption band (see Table 2).

Up to now and to the best of our knowledge, best optical-to-optical efficiencies were below 40% when using single-pass end-pumping. The maximum output powers related in this paper are, to the best of our knowledge, the highest values ever obtained under such a simple configuration, leading to significantly greater optical conversion factors. Similar efficiencies can only be reached when using more complicated pumping scheme. For example, Yb:KYW [1] provided 60% of optical conversion, while Yb:YAG exhibits 48% of optical efficiency [12] when using the thin disk configuration.

4.2   *Dependence with pump wavelength*

Both Yb-doped oxyorthosilicates seem to be good candidates for efficient, simple and low-cost multiwatt diode-pumped laser around 1 µm. An argument for this latter assertion is the test of laser performance (output power) regarding variation of the pump wavelength. Indeed, low dependence with pump wavelength can decrease constraints and complexity of the pump module. In particular, if the pump wavelength dependence is not too critical regarding the output power, the thermal regulation of the pump module can be less accurate, and then cheaper. For this purpose, we simply changed the temperature of the laser diode, then drifting its emission wavelength, and measured the obtained maximum output power. Figure 5 shows variations of the maximum output power with
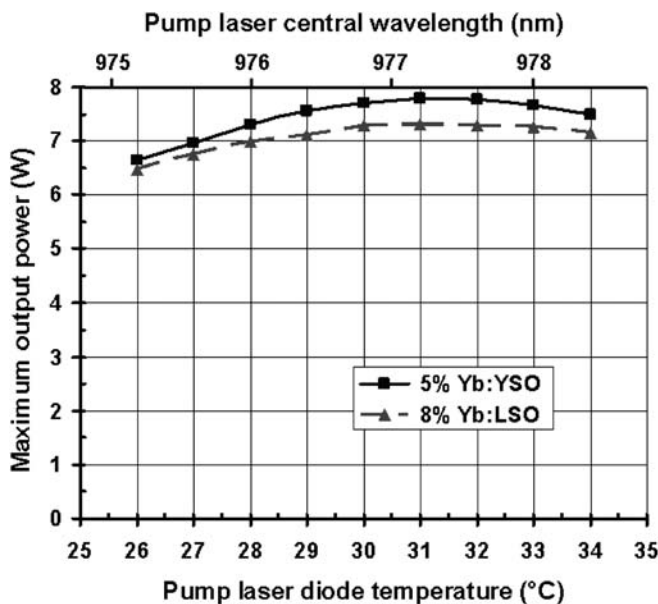
the temperature of the pump laser diode for both crystals under an incident pump power of 14.4 W.

It appears that more than 6 W of output power can be obtained over a temperature range of more than 8 °C (i.e., a shift of 3 nm for pump wavelength). Yb:LSO seems to be a little less sensitive to temperature drift, but behaviors for both crystals are quite similar. Indeed, the absorption lines of Yb:LSO are a little broader than Yb:YSO ones (4.5 nm versus 3.5 nm), but this advantage balances the drawback of smaller averaged absorption cross-sections in the X- and Z-axis. On the other hand, considering Yb:YSO, the relative narrowness of its absorption transition is partially compensated by higher absorption cross-section values. Thus, both crystals are relatively faintly sensitive regarding the pump wavelength, making them good candidates for the development of low-cost laser sources.

4.3   *Compared tunability tests*

We tuned the laser wavelength by inserting a Lyot filter into the collimated arm of the laser resonator. The Lyot filter was oriented at Brewster angle to reduce the losses for TM polarization. Both crystals are biaxial, and, as already said, placed with their X-polarization axis in the plane of the cavity, such that the X-polarized lasing mode matched the TM polarization with respect to the Lyot filter surface. Tuning curves obtained under the same conditions for Yb:LSO and Yb:YSO are shown on Fig. 6.

Tuning ranges are continuous and indeed broad for both crystals. It extends from 1025 nm to 1091 nm for Yb:YSO and from 1030 nm to 1095 nm for Yb:LSO. Yb:YSO provides more than 4 W over a bandwidth of 60 nm with a relatively flat tuning curve, while Yb:LSO exhibits more than 4 W over more than 50 nm, but with more pronounced emission peaks around 1083, 1068 and 1057 nm. In each case, the tuning range is limited on the short wavelengths by the dichroic coating of both input and folding mirrors and also by the free spectral range of the Lyot filter.

Finally, both Yb-doped silicates Yb:YSO and Yb:LSO exhibit similar laser performances, in terms of output power
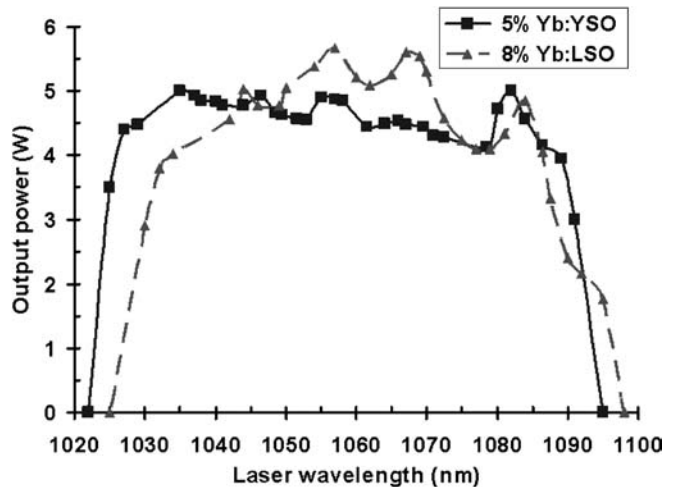
FIGURE 5   Output powers versus pump laser diode temperature for Yb:YSO and Yb:LSO at maximum incident pump power of about 14.4 W

FIGURE 6   Tuning curves obtained with a Lyot filter for Yb:YSO and Yb:LSO for 14 W of pump power

(> 7 W), optical efficiency (> 50%), tunability and sensitivity to pump wavelength drift. Nevertheless, Yb:LSO exhibits a major advantage, compared to Yb:YSO: its high thermal conductivity value does not decrease with Yb-doping rate. Then, it is possible to use shorter crystals with higher Yb-doping rates, reducing the overlap mismatch between pump beam and cavity fundamental mode, when using poor M^2 pump beams.

5   Conclusion

In conclusion, we have reported here, for the first time to the best of our knowledge, efficient laser action of two Yb-doped silicate crystals Yb:YSO and Yb:LSO under high power diode pumping. Both crystals' elaboration is now well controlled, and the crystals exhibit good thermo-optical properties. In particular, Yb:LSO offers a really good thermal conductivity value of about $5.3 \, \mathrm{W \, m^{-1} K^{-1}}$ nearly invariant with the Yb-doping rate. We obtained up to 7.7 W of laser radiation at 1082 nm for 14.4 W of incident pump power for Yb:YSO and, up to 7.3 W at 1058 nm with Yb:LSO in the same conditions. These powers provide high optical conversions of 53% and 50%, respectively for YSO and LSO. One can also add that these performances have been obtained under a simple end-pumping setup without any special thermal management of the gain media. In particular, we have shown here that these crystals exhibit comparable optical conversion efficiencies like Yb:YAG or Yb:KYW in thin disk configuration.

Moreover, both crystals are little sensitive to wavelength drift of the pump laser diode, providing more than 6 W of output power over a range of 3 nm of the central pump wavelength. In addition, large tunability curves had been obtained for both crystals. In particular, Yb:LSO provides more than 4 W of laser radiation over 50 nm (1034–1086 nm), while Yb:YSO affords more than 4 W over 60 nm (1025–1090 nm).

It then appeared that this Yb-doped silicate family offers many advantages making them really suitable for efficient, low-cost, multiwatt and tunable diode-pumped laser sources. In particular, these crystals, and especially Yb:LSO, seem to be good candidates for the development of new thin-disk high-power laser sources, since they combine easy growth, high absorption cross-sections and good thermal conductivity. Finally, even if they exhibit structured emission spectra, mode-locking these crystals should also be possible and may provide high power femtosecond laser sources, thanks to good thermo-optical properties and large emission spectra.

REFERENCES

1   S. Erhard, J. Gao, A. Giesen, K. Contag, A.A. Lagatsky, A. Abdovand, N.V. Kuleshov, J. Aus der Au, G.J. Spühler, F. Brunner, R. Paschotta, U. Keller: Trends in Optics and Photonics (TOPS), Conference on Lasers and Electro-Optics (CLEO 2001), Technical Digest, Postconference Edition 56 (Optical Society of America, Washington DC 2001), pp. 333–334

2   F. Brunner, G.J. Spühler, J. Aus der Au, L. Krainer, F. Morier-Genoud, R. Paschotta, N. Lichtenstein, S. Weiss, C. Harder, A.A. Lagatsky, A. Abdolvand, N.V. Kuleshov, U. Keller: Opt. Lett. **25**, 1119 (2000)

3   J. Petit, B. Viana, P. Goldner, D. Vivien, P. Louiseau, B. Ferrand: Opt. Lett. **29**, 833 (2004)

4   C.D. Marshall, L.K. Smith, R.J. Beach, M.A. Emanuel, K.I. Schaeffers, J. Skidmore, S.A. Payne, B.H.T. Chai: IEEE J. Quantum Electron. **QE-32**, 650 (1996)

5   F. Druon, S. Chénais, P. Raybaut, F. Balembois, P. Georges, R. Gaumé, P.H. Haumesser, B. Viana, D. Vivien, S. Dhellemmes, V. Ortiz, C. Larat: Opt. Lett. **27**, 1914 (2002)

6   S. Chénais, F. Druon, F. Balembois, G. Lucas-Leclin, P. Georges, A. Brun, M. Zavelani-Rossi, F. Augé, J-P. Chambaret, G. Aka, D. Vivien: Appl. Phys. B **72**, 389 (2001)

7   F. Druon, S. Chénais, P. Raybaut, F. Balembois, P. Georges, R. Gaumé, G. Aka, B. Viana, S. Mohr, D. Kopf: Opt. Lett. **27**, 197 (2002)

8   S. Chenais, F. Druon, F. Balembois, P. Georges, A. Brenier, G. Boulon: Opt. Mater. **22**, 99 (2003)

9   A. Lucca, M. Jacquemet, F. Druon, F. Balembois, P. Georges, P. Camy, J.L. Doualan, R. Moncorgé: Opt. Lett. **29**, 1879 (2004)

10   J. Kong, D.Y. Tang, J. Lu, K. Ueda, H. Yagi, T. Yanagitani: Opt. Lett. **29**, 1212 (2004)

11   K. Petermann, L. Fornasiero, E. Mix, V. Peters: Opt. Mater. **19**, 67 (2002)

12   C. Stewen, M. Larionov, A. Giesen, K. Contag: In OSA *Trends in Optics and Photonics – Advanced Solid-State Laser*, ed. by H. Injeyan, U. Keller, C. Marshall, Vol. 34, 35–41 (Optical Society of America, Washington DC 2000)

13   P. Raybaut, F. Druon, F. Balembois, P. Georges, R. Gaumé, B. Viana, D. Vivien: Opt. Lett. **28**, 2195 (2003)

14   Carel W.E. Van Eijk: Nucl. Instrum. Methods Phys. Res., Sect. A **392**, 285 (1997)

15   B. Comaskey, G.F. Albrecht, S.P. Velsko, B.D. Moran: Appl. Opt. **33**, 6377 (1994)

16   C. Deka, B.H.T. Chai, Y. Shimony, X.X. Zhang, E. Munin, M. Bass: Appl. Phys. Lett. **61**, 2141 (1992)

17   C.K. Chang, J.Y. Chang, Y.K. Kuo: In :Proceedings of SPIE Vol. 4914 High-Power Lasers and Applications, 498–509 (2002)

18   C. Li, R. Moncorgé, J.C. Souriau, C. Borel, C. Wyon: Opt. Commun. **107**, 61 (1994)

19   R. Gaumé, P.H. Haumesser, B. Viana, G. Aka, D. Vivien, E. Scheer, P. Bourdon, B. Ferrand, M. Jacquet, N. Lenain: Advanced Solid-State Laser **34**, 469 (2000)

20   M. Jacquemet, F. Balembois, S. Chénais, F. Druon, P. Georges, R. Gaumé, B. Ferrand: Appl. Phys. B **78**, 13 (2004)

21   B. Viana, D. Vivien, P. Loiseau, S. Jandl, S. Campos: Solid-State Lasers Proceeding of SPIE Photonics Europe 2004 **48**, 5460, (2004)

22   R. Gaumé, B. Viana, D. Vivien, J.P. Roger, D. Fournier: Appl. Phys. Lett. **83**, 1355 (2003)

23   P. Klopp, V. Petrov, U. Griebner, V. Nesterenko, V. Nikolov, M. Marinov, M.A. Bursukova, M. Galan: Opt. Lett. **28**, 322 (2003)